

# A Framework for Fast and Efficient Neural Network Compression

Hyeji Kim, Muhammad Umar Karim, and Chong-Min Kyung  
School of Electrical Engineering, KAIST, Republic of Korea

*Abstract*—Network compression reduces the computational complexity and memory consumption of deep neural networks by reducing the number of parameters. In SVD-based network compression, the right rank needs to be decided for every layer of the network. In this paper, we propose an efficient method for obtaining the rank configuration of the whole network. Unlike previous methods which consider each layer separately, our method considers the whole network to choose the right rank configuration. We propose novel accuracy metrics to represent the accuracy and complexity relationship for a given neural network. We use these metrics in a non-iterative fashion to obtain the right rank configuration which satisfies the constraints on FLOPs and memory while maintaining sufficient accuracy. Experiments show that our method provides better compromise between accuracy and computational complexity/memory consumption while performing compression at much higher speed. For VGG-16 our network can reduce the FLOPs by 25% and improve accuracy by 0.7% compared to the baseline, while requiring only 3 minutes on a CPU to search for the right rank configuration. Previously, similar results were achieved in 4 hours with 8 GPUs. The proposed method can be used for lossless compression of neural network as well. The better accuracy and complexity compromise, as well as the extremely fast speed of our method makes it suitable for neural network compression.<sup>1</sup>

## I. INTRODUCTION

Deep convolutional neural networks have been consistently showing outstanding performance in a variety of applications, however, this performance comes at a high computational cost compared to past methods. The millions of parameters of a typical neural network require immense computational power and memory for storage. Thus, model compression is required to reduce the number of parameters of the network. Our aim in this paper is to develop a method that can optimize trained neural networks for reduction in computational power and memory usage while providing competitive accuracy.

Generally, filter pruning techniques have been used for network compression. The aim of such approaches to develop pruning policies, which can satisfy the target constraints on FLOPs and memory. Layer wise search-based heuristic methods [1]–[3], reinforcement learning [4]–[6], and genetic and evolutionary algorithms [7], [8] have been used to define the pruning policy. A greedy selection method based on heuristic metric has been proposed in [9], [10] to prune multiple filters of the network together.

Another approach towards network compression is using kernel decomposition over each filter in the network. Convolutional and fully connected layers can be represented as matrix

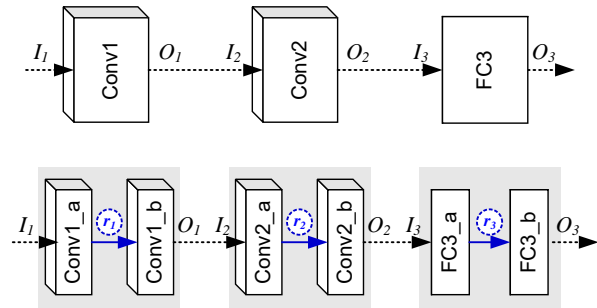


Fig. 1. Kernel decomposed convolution and fully-connected layers. Each layer is split into two with low-rank decomposition.

multiplications, and kernel decomposition can be applied to these matrices [11]–[16]. Kernel decomposition with singular value decomposition (SVD) automatically assigns importance (the singular values) to the decomposed kernels. This automatic sorting makes filter pruning easier, as the decomposed kernels with the lower parameters are the first to be pruned. Simply put, the low-rank approximations of the layers are decomposed into two matrices for network compression as shown in Fig. 1.

With kernel decomposition schemes, the problem boils down to the choice of the right rank for each layer of the network. In other words, we need to find the rank configuration for the whole network that satisfies constraints on speed, memory and accuracy. In [16], the authors define an accuracy feature and find the right rank for each layer to maximize this feature. Reinforcement learning was used in [17] to find the rank of each layer independently. An iterative search-based approach was adopted in [18] to obtain the right rank configuration. Unlike [16] and [17], which optimize each layer separately, [18] searched for the right rank configuration for the whole network. Although, [18] shows better performance compared to [16] and [17], it still takes significant amount of time due to its iterative search for the right rank configuration.

In this paper, we propose Efficient Neural network Compression(ENC) to obtain the optimal rank configuration for kernel decomposition. The proposed method is non-iterative; thereby, it performs compression much faster compared to numerous recent methods. Specifically, we propose three methods: ENC-Map, ENC-Model and ENC-Inf. ENC-Map uses a mapping function to obtain the right rank configuration from the given constraint on complexity. ENC-Model uses a metric representative of the accuracy of the whole network

Email: hyejikim89@kaist.ac.kr

<sup>1</sup>Code will be released to public upon acceptance of this work.

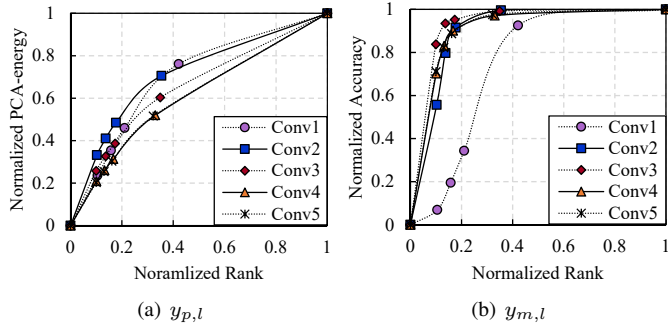


Fig. 2. Interpolated function of layer-wise accuracy metric in AlexNet. (a)  $y_{p,l}$  based on normalized PCA energy. (b)  $y_{m,l}$  based on normalized accuracy using partial training dataset.

to find the right rank configuration. ENC-Inf uses both the accuracy model and inference on a partial dataset to arrive at the right rank configuration.

The rest of the paper is structured as follows. Section 2 and 3 describe the accuracy metrics. Section 4 discusses ENC-Map. Search-based methods, ENC-Model and ENC-Inf, are given in Section 5. Experiments are discussed in Section 6 and Section 7 concludes the paper.

## II. LAYER-WISE ACCURACY METRICS

The error of the neural network can be divided over the constituent layers of the network. In other words, each layer contributes to the error or accuracy of the neural network. The accuracy contributed by a layer is a function of the complexity or rank of that layer. In this section, we describe a couple of metrics, which can be used to predict the contribution of an individual layer to overall accuracy of the network. The first metric is based on heuristics while the second involves computing the accuracy over a partial dataset.

After singular value decomposition (SVD), the number of principal components retained directly affects the complexity as well as the accuracy. Let us define the un-normalized PCA energy as

$$\sigma'_l(r_l) = \sum_{d=1}^{r_l} \sigma_l(d), \quad (1)$$

where  $r_l$  is the rank of the  $l$ -th layer in the neural network and  $\sigma_l(d)$  is the  $d$ -th singular value after performing SVD on the parameters on  $l$ -th layer. In detail,  $\sigma'_l(r_l)$  is the sum of the first  $r_l$  diagonal entries of the diagonal matrix after decomposition. It is obvious that the accuracy decreases with the decrease in un-normalized PCA energy. The PCA energy of the  $l$ -th layer at with a rank  $r_l$  is obtained by performing min-max normalization to the un-normalized PCA energy, i.e.,

$$y_{p,l}(r_l) = \frac{\sigma'_l(r_l) - \sigma'_l(1)}{\sigma'_l(r_l^{max}) - \sigma'_l(1)}. \quad (2)$$

Here  $r_l^{max}$  is the maximum or initial rank.

The second metric for layer-wise accuracy that we use in this paper is based on evaluation of the neural network on a partial dataset. For the  $l$ -th layer, the accuracy model is obtained by changing  $r_l$  while keeping the rest of the

network unchanged. Empirical models are developed for each layer. Note that the possible number of ranks for a layer occupy a large linear discrete space, making it impractical to evaluate the accuracy over the partial dataset. Therefore, we use VBMF [19] to sample ranks over which the accuracy is estimated and follow it up by Piecewise Cubic Hermite Interpolating Polynomial (PCHIP) algorithm. We denote the measurement-based layer-wise accuracy metric of the  $l$ -th layer by  $y_{m,l}(r_l)$ .

In Fig. 2, we show the result of interpolation with both the PCA energy-based and measurement-based approaches. Both the metrics show different profiles. It is because the PCA energy is not a representation of accuracy in itself but monotonic with the overall accuracy.

## III. ESTIMATING ACCURACY WITH THE INDEPENDENCE ASSUMPTION

In this section, we describe how we can use the previously defined layer-wise metrics to represent the accuracy of the complete neural network. We estimate the joint distribution of the output of the neural network and the configuration of its layers. The configuration of the layers of the neural network is defined only by the choice of the rank for each layer.

Our aim is to maximize the accuracy of the network with a given set of constraints. Let us define the configuration of a neural network through the rank configuration, which is a set of ranks of each layer, i.e.,

$$R = \{r_1, r_2, \dots, r_L\}, \quad (3)$$

where  $r_n$  is the rank of the  $n$ -th layer. The overall accuracy of the network can be represented by the joint distribution of accuracy of individual layers. Precisely,

$$P(A; R) = P(a_1, a_2, \dots, a_L; R), \quad (4)$$

where  $a_n$  is the accuracy provided by the  $n$ -th layer. Here we make a simplifying assumption that the accuracy contribution of a layer is a function of the rank of the layer only. Practically, the accuracy contribution of a layer also depends on the ranks of other layers. However, such independence assumptions have been used in the past as well, for example the Naive Bayes' method, and have shown decent results. Based on this assumption, we can write

$$P(A; R) = \prod_{l=1}^L P(a_l; r_l). \quad (5)$$

This representation of accuracy has been inspired by [16] where the product of layer-wise accuracy metrics is used to estimate the overall accuracy.

The metrics defined for representing the layer-wise accuracy can be used in (5). The metric based on the measured accuracy can be directly used to replace  $P(a_l; r_l)$ , i.e.,

$$A_m(R) = \prod_{l=1}^L y_{m,l}(r_l) \quad (6)$$

estimates the overall accuracy of the network based on the measured accuracy over a partial dataset. The PCA energy of

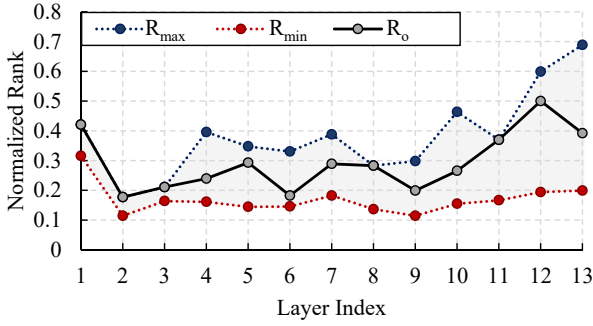


Fig. 3. Space boundaries from  $R_{max}$  and  $R_{min}$  in VGG-16 ( $C_t=25\%$ ,  $\delta_s=\pm 10\%$ ). A final rank configuration  $R_o$  is selected among the candidate rank configurations generated within these boundaries.

(2) cannot be directly used as accuracy. However, it was shown in [16] that the PCA energy of a layer is directly proportional to the accuracy of the network. Thus, we can write

$$A_p(R) \propto \prod_{l=1}^L y_{p,l}(r_l). \quad (7)$$

As will be seen shortly, we are not interested in the exact value of the estimated accuracy but rather the rank configurations of the neural network that provide the maximum accuracy. In other words, we assume that the accuracy and the PCA energy only have a scale difference, and their maximas lie at the same points. Finally, we define a combined metric for representing the accuracy of the whole neural network. This metric takes into consideration both the PCA energy and the measurement based layer-wise accuracy metrics. Mathematically,

$$A_c(R) = \left\{ \prod_{l=1}^L y_{p,l}(r_l) \times \sum_{l=1}^L \frac{C_l(r_l)}{C_{orig}} \right\} + \prod_{l=1}^L y_{m,l}(r_l), \quad (8)$$

where  $C_l(r_l)$  is the complexity of the  $l$ -th layer and  $C_{orig}$  is the total complexity of the network. The complexity  $C_l(r_l)$  is defined by  $c_l r_l$ , where  $c_l$  for spatial decomposition is

$$c_l = W_l H_l D_l (I_l + O_l) / s_l^2 \quad (9)$$

and for channel decomposition

$$c_l = W_l H_l (I_l D_l^2 + O_l) / s_l^2. \quad (10)$$

Here  $W_l$  and  $H_l$  are the width and height of feature map,  $D_l$  is the size of filter window,  $I_l$  and  $O_l$  are the number of input channels and filters,  $s_l$  is the stride. Refer to [12] and [11] for spatial and channel decomposition, respectively. Also,

$$C(R) = \sum_{l=1}^L C_l(r_l). \quad (11)$$

In our experiments, we have noticed that the PCA energy metric does not accurately represent the accuracy at lower complexities; therefore, we have weighted the PCA energy with the complexity.

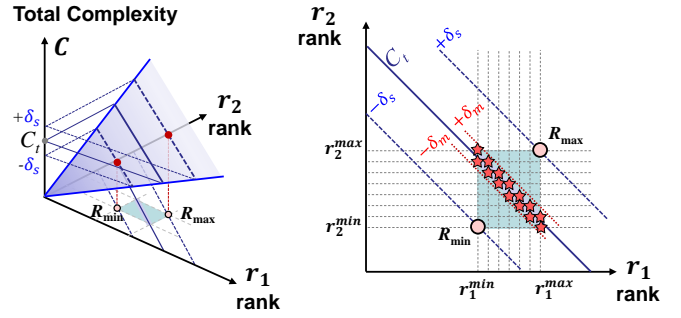


Fig. 4. Combinatorial space generation for target complexity  $C_t$  (as an example of two-layered CNN). When the space margin  $\pm \delta_s$  is applied to  $C_t$ , the effective rank-set space is defined by the upper and lower boundaries of ranks  $R_{max}$ ,  $R_{min}$ . The rank-sets satisfying  $C_t \pm \delta_m$  are extracted as the candidate rank-sets.

#### IV. RANK CONFIGURATION WITH ACCURACY-COMPLEXITY MAPPING

In this section, we present a simple method to choose the rank configuration for a neural network by mapping complexity against accuracy. The mapping is performed through the rank configurations, as both complexity and accuracy are functions of rank configurations. A complete mapping of the complexity of the network against the accuracy metrics is impractical due to the large number of possible rank configurations. Therefore, we only consider the rank configurations for which layer-wise rank metrics are equal for every layer. Mathematically,

$$R_e = R \mid y_{i,l}(r_l) = y_{i,k}(r_k), \quad (12)$$

where  $l, k \in 1, 2, \dots, L$  and  $i \in \{p, m\}$ . Next the total complexity  $C(R_e)$  is computed using (11). The accuracy and complexity are plotted against each other over  $R_e$ , which provides a mapping between complexity and the accuracy. The mapping is mathematically given as

$$f_{C-A} : \mathbb{R} \rightarrow \mathbb{R}. \quad (13)$$

Also note that the mappings from complexity and accuracy to the rank configuration and vice versa do exist as well, i.e.,

$$f_{C-R} : \mathbb{R} \rightarrow \mathbb{R}^L. \quad (14)$$

Using this mapping, the achievable accuracy and the respective rank configuration can be obtained while satisfying constraints on complexity. This method is called ENC-Map as we use a simple mapping to obtain the right rank configuration.

#### V. COMBINATORIAL SEARCH FOR RANK CONFIGURATION

The method described in the previous section strongly depends on the layer-wise metrics. These metrics are simple estimates for the accuracy. Therefore, it is logical to search a region in the rank configuration space to choose the rank configuration.

To limit the space for the combinatorial search, we perform two steps. First, we limit the search space by determining the boundaries. Then, we conduct the search in the limited space.

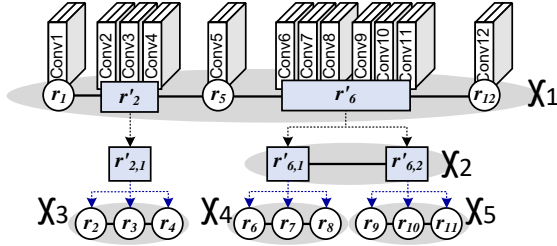


Fig. 5. Hierarchical space generation (as an example of 12-layered network). There are 3 hierarchy level and five sub-spaces ( $\mathcal{X}_1, \dots, \mathcal{X}_5$ ). The maximum space complexity is  $\mathcal{O}(n^5)$  of  $\mathcal{X}_1$ .

### A. Limiting the Search Space

It is impossible to search over the whole rank configuration space for the optimal rank configuration. To limit the search space, we use the simple method described in the previous section. We obtain the upper bound on the search space by using the mapping in (14)

$$R_{max} = f_{C-R}(C_t + \delta_s) \quad (15)$$

and the lower bound by

$$R_{min} = f_{C-R}(C_t - \delta_s). \quad (16)$$

Here  $C_t$  is the complexity constraint and  $\delta_s$  is the space margin. As illustrated in Fig. 3, the final rank configuration  $R_o$  satisfying the target complexity is selected within the space boundaries  $R_{max}$  and  $R_{min}$ .

### B. Min-offsetting the Search Space

In the limited space by the  $R_{max}$  and  $R_{min}$ , we are only interested in the candidate rank configurations as

$$\mathbf{R} = \bigcup R \mid C_t - \delta_m < C(R) < C_t + \delta_m, \quad (17)$$

for  $R \in [R_{min}, R_{max}]$ . These candidate rank configurations satisfy the target complexity  $C_t$  with marginal error  $\pm \delta_m$ . To simplify the search space, we shift the space boundaries from  $[R_{min}, R_{max}]$  to  $[0, R_{max} - R_{min}]$ . Then, we generate the differential search space and extract the differential candidate rank configurations  $\hat{\mathbf{R}}$  defined by

$$\hat{\mathbf{R}} = \bigcup R \mid \Delta C_t - \delta_m < C(R) < \Delta C_t + \delta_m, \quad (18)$$

for  $\Delta C_t = C(R_{max}) - C_t$  and  $R \in [0, R_{max} - R_{min}]$ . Note that  $\mathbf{R} = R_{max} - \hat{\mathbf{R}}$ .

### C. Hierarchical Space Generation

To reduce the complexity of space generation and to generate a denser search space, we hierarchically generate the sub-spaces by grouping some layers and extract only the candidate rank configurations in top-down manner as illustrated in Fig. 5.

As denoted in 11, the total complexity is the function of rank configuration  $C(R) = \sum_l c_l r_l$ . In the min-offset search space, the range of all ranks start from zero, so that we can simply gather some dimension for rank such as  $\sum_i c_i r_i$  to  $c'_i r'_i$  with the newly defined  $c'_i$  and  $r'_i$ . The range of  $r'_i$  is defined in

### Algorithm 1 : Optimal Rank Configuration

---

**INPUTS:**  $h \leftarrow$  A neural network,  $C_t \leftarrow$  Target complexity,  $method \leftarrow$  ENC-Map, ENC-Model, ENC-Inf  
**OUTPUT:**  $R_o \leftarrow$  Rank configuration  
**Parameters:**  $\delta_s \leftarrow$  Parameter for limiting the search space,  $\delta_m \leftarrow$  Parameter for marginal error of  $C_t$ ,  $N \leftarrow$  Number of rank configurations for evaluation

//Layer-wise metrics  
 Compute  $y_{p,l}, y_{m,l}$  for all  $l \in 1 \dots L$   
 Compute  $f_{C-A}, f_{C-R}$   
**if**  $method ==$  ENC-Map **then**  
      $R_o = f_{C-R}(C_t)$   
**else**  
     //Candidate rank-set generation  
      $R_{max} = f_{C-R}(C_t + \delta_s)$   
      $R_{min} = f_{C-R}(C_t - \delta_s)$   
      $\mathbf{R} = \{\cup R \mid C_t - \delta_m < C(R) < C_t + \delta_m\}$   
         for  $R \in [R_{min}, R_{max}]$   
     //Accuracy estimate for the  
     //whole neural network  
     Compute  $A$  of  $\mathbf{R}$   
     **if**  $method ==$  ENC-Model **then**  
          $R_o = \arg \max_R A(R)$  s.t.  $R \in [R_{min}, R_{max}]$   
     **else if**  $method ==$  ENC-Inf **then**  
         Compute  $\mathbf{R}_A \in \mathbb{R}^{N \times L}$   
         Evaluate accuracy of each row of  $\mathbf{R}_A$  over  
         the partial dataset  
         Select  $R_o$  from  $\mathbf{R}_A$  with best evaluation  
     **end if**  
**end if**

---

$[0 : \min(\{t_i\}) : r'_{i,max}]$  where  $t_i$  is the interval size of range for a rank  $r_i$ . The definition of maximum  $r'_{i,max}$  is different based on the grouping rule: (i) gathering by the same layer complexity  $c_i$  and  $r'_{i,max} = \sum \max(\{r_i\})$ , (ii) gathering by the  $r_i$  and  $c'_i = \sum_i c_i$ ,  $r'_{i,max} = \max(\{r_i\})$ . In our experiments, we use the grouping rule (i).

The density of space is directly related to the probability of finding the optimal rank configuration. Since most search time comes from generating  $\mathbf{R}$ , the hierarchical space generation can save significant time. Therefore, when the space complexity is simpler, we can make the space denser. We define the average density of the vector space for each rank  $r_l$  as  $\delta_d = \sum_l 1/(t_l L)$ . Here, the range of rank in min-offset space is represented with the vector space and the  $t_l$  means the sampling period of vector space.

An example of 12-layered CNN is illustrated in Fig. 5. There are 3-hierarchical levels for space grouping and 5 types of sub-spaces, which are  $[\mathcal{X}_1, \dots, \mathcal{X}_5]$ . The number of dimensions in a group determines the complexity of sub-space. By the hierarchical grouping, the maximum space complexity is reduced from  $\mathcal{O}(n^{12})$  to  $\mathcal{O}(n^5)$  in  $\mathcal{X}_1$ .

### D. Choice of Rank Configuration

Apart from the simple method described in Section IV, we use two methods for obtaining the optimal rank configuration

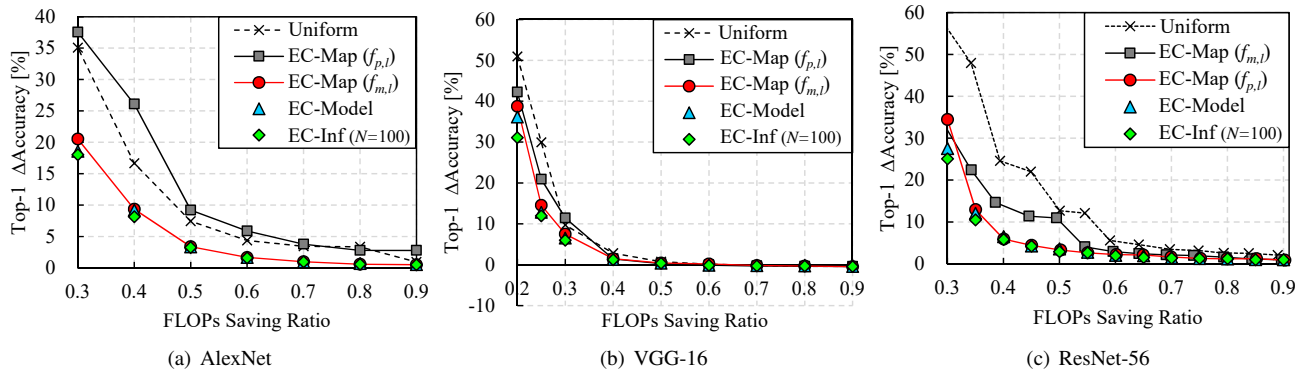


Fig. 6. Performance comparison of overall accuracy metrics. Baseline top-1 accuracy is 56.6% for AlexNet, 70.6% for VGG-16, and 93.1% for ResNet-56. Smaller  $\Delta$  Acc. is better.

for a given neural network. For both the methods, we choose a subset  $\mathbf{R}$  of rank configurations in 17. In detail,  $\mathbf{R}$  includes the rank configurations for which the complexity is roughly equal to  $C_t$ . Note that we slightly expand the search space by using the parameter  $\delta_m$ .

In the first method, we choose a rank configuration that maximizes  $A(R)$  which is one of  $A_m(R)$ ,  $A_p(R)$ ,  $A_c(R)$  denoted in (6, 7, 8). I.e.,

$$R_o = \arg \max_R A(R) | R \in \mathbf{R} \quad (19)$$

This method is called ENC-Model.

In the second method, we choose  $N$  rank configurations, which provide the largest values of (8). These  $N$  rank configurations are stored in  $\mathbf{R}_A$  and then evaluated over the partial dataset to choose the best rank configuration.

The complete process is given in Algorithm 1. ENC-Map provides a quick and dirty solution, whereas ENC-Model and ENC-Inf approaches are relatively slower. However, even our slowest method easily outperforms state-of-the-art approaches in speed.

The proposed method can be used to both reduce the FLOPs or the memory consumption of the neural network. The constraint  $C_t$  can represent both the number of FLOPs or the number of parameters of the neural network.

Our proposed methods can provide rank configurations under both complexity and accuracy constraints. Till now, the discussion followed complexity constrained systems. In other words, given a complexity constraint our aim is to obtain a rank configuration that maximizes the accuracy. However, shifting to accuracy constrained systems is straightforward. Given an accuracy constraint, we use the inverse mapping of  $f_{C-A}$ ,  $f_{A-C}$ , to obtain the complexity corresponding to a given accuracy. The obtained complexity is input to the Algorithm 1 to obtain the rank configuration.

## VI. EXPERIMENTAL RESULTS

In this section, we present the experimental evaluation of the proposed methods. We first present a comparison of the proposed methods. We discuss the scenarios that dictate the choice of any of the proposed methods. Afterwards, we

compare the proposed methods against some recently proposed neural network optimizing methods.

For our experiments, we have optimized the AlexNet [20], VGG-16 [21] and ResNet-56 [22] networks. For AlexNet and VGG-16, we have used the ImageNet [23] dataset. For ResNet-56, we have used the Cifar-10 [24] dataset. We have performed the same pre-processing (image cropping and resizing) as described in the original papers [20]–[22]. Also, we have used 4% and 10% of the ImageNet and Cifar-10 training datasets as the partial datasets.

The parameters  $\delta_s$  and  $\delta_m$  were set to 10% of the original total complexity and 0.5% of the target complexity, respectively. We use  $N = 50$  with AlexNet, and  $N = 20$  with both VGG-16 and ResNet-56. For ENC-Model and ENC-Inf, we use the accuracy metric  $A_m(R)$  as  $A(R)$  for AlexNet,  $A(R)$  for VGG-16, and  $A_p(R)$  as  $A(R)$  for ResNet-56. Also, note that we have performed channel decomposition to the first layer whenever required and spatial decomposition to the rest of the layers using truncated SVD. For VGG-16, the first layer was decomposed to half the original rank following [18] and for ResNet-56, the first layer was not decomposed at all.

The experiments were conducted on a system with four Nvidia GTX 1080ti GPUs and Intel Zeon E5-2620 CPU. The experiments conducted on the CPU used a single core and code optimization was not performed. The *Caffe* [25] library was used for development.

### A. Comparison of Layer-wise accuracy metrics

This section presents the comparison of the two layer-wise accuracy metrics based on the results of the fast method. The results are shown in Fig. 6. We note that the PCA energy-based metric shows poor performance with the shallower AlexNet. This is expected as the PCA energy is not based on actual inference and expected to show poorer performance compared to the measurement-based layer-wise accuracy metric. However, with the deeper VGG-16 and ResNet-56, the performance of PCA energy-based and the measurement-based layer-wise accuracy metric is almost same. The reason is that the complexity difference from rank reduction on each layer is less as the layer is deeper, so that the accuracy

TABLE I  
PERFORMANCE COMPARISON OF NETWORK COMPRESSION TECHNIQUES. SMALLER  $\Delta$ ACC. IS BETTER.

| Model                                   | Target Complexity                       | Searching Policy       | Top-1/Top-5 $\Delta$ Acc. [%] |                    | Search Time                 |
|---|---|------------------------|-------------------------------|--------------------|-----------------------------|
|   |   |                        | w/o FT                        | w/ FT              |                             |
| AlexNet<br>(56.6% / 79.9%)<br>@ImageNet | FLOPs 37.5%<br>Parameters 18.4%<br>[13] | Y-D <i>et al.</i> [13] | - / -                         | - / 1.6            | -                           |
|   |   | <b>ENC-Inf</b>         | - / -                         | <b>-0.1 / -0.2</b> | <b>3m @4GPUs</b>            |
|   |   | ENC-Model              | - / -                         | -0.1 / -0.2        | 1m @CPU                     |
| VGG-16<br>(70.6 / 89.9)<br>@ImageNet    | FLOPs 25%                               | Uniform                | 29.9 / 23.6                   | 0.8 / 0.5          | -                           |
|   |   | Heuristic [17]         | - / 11.7                      | - / -              | -                           |
|   |   | ADC [17]               | - / 9.2                       | - / -              | 4h @8GPUs                   |
|   |   | ARS [18]               | 13.0 / 9.1                    | -0.3 / -0.1        | 7h @4GPUs<br>(in our impl.) |
|   |   | <b>ENC-Inf</b>         | <b>10.7 / 7.3</b>             | <b>-0.6 / -0.2</b> | <b>5m @4GPUs</b>            |
|   |   | ENC-Model              | 11.3 / 7.9                    | -0.7 / -0.2        | 3m @CPU                     |
| ResNet-56<br>(93.1% / -)<br>@Cifar-10   | FLOPs 50%                               | ENC-Map                | 14.5 / 10.2                   | -0.2 / -0.1        | 3.4s @CPU                   |
|   |   | Uniform                | 12.7 / -                      | 0.2 / -            | -                           |
|   |   | AMC [4]*               | 2.7* / -                      | 0.9* / -           | 1h @GPU                     |
|   |   | <b>ENC-Inf</b>         | <b>2.9 / -</b>                | <b>0.1 / -</b>     | <b>3m @4GPUs</b>            |
|   |   | ENC-Model              | 3.5 / -                       | 0.1 / -            | 1m @CPU                     |
| ENC-Map                                 | 3.3 / -                                 | 0.1 / -                | 2.9s @CPU                     |                    |                             |

\* Baseline accuracy of [4] is 92.8%.

difference is also smaller. The measurement-based metric can not completely represent the overall accuracy.

The PCA energy-based and measurement-based metrics require 5 seconds and 5 minutes for ResNet-56. Note that once these metrics are evaluated, they can be used for different complexity. For every new neural network that needs to be optimized, these metrics need to be evaluated beforehand.

### B. Comparison of the Fast, Search without Inference and Search with Inference Methods

In this section, we compare the performance of ENC-Map, ENC-Model and ENC-Inf against each other. The results are shown in Fig. 6. It is seen that at lower compression (or relatively higher complexity requirements), the performance of all the three methods is almost the same. However, at higher compression, the performance of ENC-Map is lower than ENC-Model and ENC-Inf. The time taken by each model is given in Table VI.

### C. Performance Comparison with Other Methods

The overall results are summarized in Table. VI. Here we use the decrease in accuracy (*i.e.*  $\Delta$ Acc.), which is the difference of accuracy of the original and optimized neural networks, as a metric to evaluate different methods. Lower decrease in accuracy is desired. Also, we mention the results with uniform rank reduction, which applies the same rank reduction ratio to every layer of the neural network. In Table. VI, the proposed methods, uniform, [17], heuristic in [17], and [18] use the SVD based spatial decomposition. [13] uses the Tucker decomposition based channel decomposition. [4] uses the channel pruning.

In [13], the authors show the compression results for FLOPs and parameters. It is not possible to use ENC-Map under both these constraints as it provides mapping only from one of these

TABLE II  
COMPARISON OVER TARGET COMPLEXITY OF 20% FLOPs WITH VGG-16. BASELINE TOP-5 ACCURACY IS 89.9%

| VGG-16<br>(FLOPs 20%)  | Top-5<br>$\Delta$ Acc. | Search Range   |
|------------------------|------------------------|----------------|
| Asym.3D [11]           | 1.0%                   | Layer-by-layer |
| Y-D <i>et al.</i> [13] | 0.5%                   |                |
| CP-3C [1]              | 0.3%                   |                |
| <b>ENC-Inf</b>         | <b>0.0%</b>            | Whole-network  |

constraints to the accuracy. However, ENC-Model and ENC-Inf can be used by populating  $\mathbf{R}$  by rank configurations that satisfy both the FLOPs and parameters constraints. We have used  $N = 50$  here and optimize both convolution and fully-connected layers. The space complexity is  $\mathcal{O}(n^7)$  excluding first convolution layer, and the average density  $\delta_d$  is 25%. Initial learning rate of  $10^{-3}$  was used, which was reduced by a factor of 2 after every 2 epochs till the 16-th. Fine tuning takes around 9 hours. As denoted in Table. VI, our method shows 1.8% higher top-5 accuracy than [13] at the same complexity. To find the rank configuration, our algorithm only takes only a minute with a single core CPU with ENC-Model and 3 minutes on 4 GPUs with ENC-Inf.

For the VGG-16 neural network, we optimize the convolution layers with FLOPs constraint. The complexity constraint is set as 25% and 20% FLOPs to compare with [17], [18] and [1], [13], [16], respectively. For the generation of combinatorial space, we use 2-level hierarchical space grouping. By gathering each Conv7-8, Conv9-10 and Conv11-13 as the three top-groups, the maximum space complexity is reduced from  $\mathcal{O}(n^{12})$  excluding Conv1 to  $\mathcal{O}(n^8)$ . The average density  $\delta_d$  is 21%. The compressed neural network was fine tuned with an initial learning rate of  $10^{-5}$ , which was decreased by a factor of 10 at the fourth epoch. Fine tuning takes about 1 day. With 25% FLOPs reduction, ENC-Inf takes only 5 minutes

TABLE III  
LOSSLESS COMPRESSION WITH FULL FINE-TUNING.

| Model     | Searching Policy | FLOPs | Top-1 $\Delta$ Acc. |
|-----------|------------------|-------|---------------------|
| AlexNet   | ENC-Inf          | 31%   | 0.0%                |
| VGG-16    | ENC-Model        | 24%   | -0.4%               |
| ResNet-56 | ENC-Map          | 55%   | -0.1%               |

TABLE IV  
AGGRESSIVE FLOPs REDUCTION WITH BRIEF FINE-TUNING FOR LOSSLESS COMPRESSION OF VGG-16.

| Searching Policy | Fine-tuning Epochs | FLOPs      | Top-1 $\Delta$ Acc. |
|------------------|--------------------|------------|---------------------|
| ADC [17]         | 0                  | 64%        | 0.0%                |
| <b>ENC-Model</b> | <b>0</b>           | <b>57%</b> | <b>-0.1%</b>        |
|                  | 0.1                | 41%        | -0.1%               |
| <b>ENC-Model</b> | 0.2                | 39%        | -0.1%               |
|                  | <b>1</b>           | <b>33%</b> | <b>0.0%</b>         |

at 4 GPUs, and it shows the 2.3% and 0.3% higher top-1 accuracy without and with fine-tuning, respectively, compared to [18]. As summarized in Table. VI, our  $\mathcal{O}(1)$  algorithm called ENC-Map is extremely fast. It can find the result with only 3.4 seconds at single core CPU, while the previous research takes 4 hours at 8 GPUs [17] and 7 hours at 4 GPUs [18]. The accuracy loss can be simply recovered with fine-tuning. Results with 20% FLOPs reduction are given in Table. II. It is seen that our method outperforms methods based on different strategies.

With the ResNet-56 neural network, we use the 3-level hierarchical layer grouping for convolution layers. At the top-view, there are five layers, which are composed by [Conv2-19, Conv20, Conv21-37, Conv38, Conv39-55] excluding first convolution layer (Conv1) and fully-connected layer. Then, we gather the hierarchical sub-groups within the limited maximum space complexity according to the number of top groups. As a result, the total space complexity is efficiently reduced from  $\mathcal{O}(n^{54})$  to  $\mathcal{O}(n^5)$ . The average density  $\delta_d$  is 70%. The compressed ResNet-56 is fine-tuned with an initial learning rate of  $10^{-3}$ , which is reduced by a factor of 10 at the 16th, 24th and 32nd epoch. Fine tuning takes around 1 hour. ENC-Map and ENC-Model achieve a 0.1% accuracy loss (*i.e.* 93.1% top-1 accuracy) with 50% FLOPs reduction after fine-tuning. The times taken by ENC-Map and ENC-Inf are 2.9 seconds with single core CPU and 5 minutes with 4 GPUs, respectively. It is most efficient searching compared to the learning based state-of-the-art, which takes 1 hour in single GPU [4].

#### D. Lossless Compression

The idea of lossless compression is to set the target accuracy to that of the original neural network and then optimize the network. However, since we use fine-tuning after optimization, we can set the target accuracy to slightly lower than that of the original neural network. The remaining accuracy is recovered by fine tuning. To set the reduced accuracy constraint, we use the method in [18]. As summarized in Table. III, our

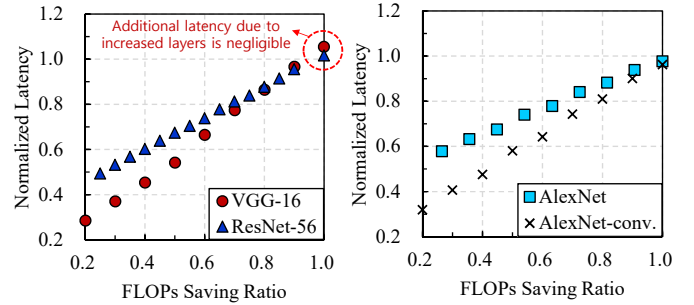


Fig. 7. Normalized CPU latency of optimized models. The latency of baseline CNN is 10.59s in VGG-16, 142.2ms in ResNet-56, and 825.0ms in AlexNet for single image classification.

compression methods achieve the significant reduction in FLOPs without accuracy loss.

The combination of our fast compression method and brief fine-tuning can aggressively reduce the FLOPs without accuracy loss. Table. IV shows the result of aggressive FLOPs reduction with fine-tuning. The accuracy thresholds considering the fine-tuning are calculated for [0.1, 0.2, 1, 5] epochs using the method in [18]. We reduced the FLOPs by 41% with VGG-16 without any accuracy loss. The process took only 0.1 epoch for 22 minutes with single GPU. Also, our method with 1 epoch fine-tuning takes 3.7 hours with single GPU, and it shows better FLOPs saving (33% FLOPs) compared to 4 hours searching (64% FLOPs) [17].

#### E. Results on an Embedded Board

We evaluate the latency of compressed network models for inference on the ODROID-XU4 board with Samsung Exynos5422 mobile processor composed of 4 ARM Cortex-A15 and 4 Cortex-A7. Fig. 7 shows that the FLOPs saving ratio in our paper is directly related to the real latency of single image inference.

We use ENC-Model for optimizing the convolution layers of AlexNet, VGG-16, and ResNet-56 in Fig. 7. We note that, the latency of convolution layers is 72% and 62% of total latency for the baseline ResNet-56 and AlexNet, respectively. Other operations include batch normalization and fully-connected layers. We also show the results of AlexNet-conv, which only considers the latency of convolution layers.

## VII. CONCLUSION

We propose efficient neural network compression methods in this paper. Our methods are based on low-rank kernel decomposition. We propose a holistic, model-based approach to obtain the rank configuration that satisfies the given set of constraints. Our method can compress the neural network while providing competitive accuracy. Moreover, the time taken by our method for compression is in seconds or minutes, whereas previously proposed methods take hours to achieve similar results.

## REFERENCES

- [1] Yihui He, Xiangyu Zhang, and Jian Sun. Channel pruning for accelerating very deep neural networks. In *International Conference on Computer Vision (ICCV)*, volume 2, 2017.
- [2] Hao Li, Asim Kadav, Igor Durdanovic, Hanan Samet, and Hans Peter Graf. Pruning filters for efficient convnets. *arXiv preprint arXiv:1608.08710*, 2016.
- [3] Jian-Hao Luo, Jianxin Wu, and Weiyao Lin. Thinet: A filter level pruning method for deep neural network compression. *arXiv preprint arXiv:1707.06342*, 2017.
- [4] Yihui He, Ji Lin, Zhijian Liu, Hanrui Wang, Li-Jia Li, and Song Han. Amc: Automl for model compression and acceleration on mobile devices. In *Proceedings of the European Conference on Computer Vision (ECCV)*, pages 784–800, 2018.
- [5] Anubhav Ashok, Nicholas Rhinehart, Fares Beainy, and Kris M Kitani. N2n learning: Network to network compression via policy gradient reinforcement learning. Apr 2018.
- [6] Han Cai, Tianyao Chen, Weinan Zhang, Yong Yu, and Jun Wang. Reinforcement learning for architecture search by network transformation. *arXiv preprint arXiv:1707.04873*, 2017.
- [7] Esteban Real, Alok Aggarwal, Yanping Huang, and Quoc V Le. Regularized evolution for image classifier architecture search. *arXiv preprint arXiv:1802.01548*, 2018.
- [8] Hanxiao Liu, Karen Simonyan, Oriol Vinyals, Chrisantha Fernando, and Koray Kavukcuoglu. Hierarchical representations for efficient architecture search. *arXiv preprint arXiv:1711.00436*, 2017.
- [9] Ting-Wu Chin, Cha Zhang, and Diana Marculescu. Layer-compensated pruning for resource-constrained convolutional neural networks. *arXiv preprint arXiv:1810.00518*, 2018.
- [10] Shaohui Lin, Rongrong Ji, Yuchao Li, Yongjian Wu, Feiyue Huang, and Baochang Zhang. Accelerating convolutional networks via global & dynamic filter pruning. In *IJCAI*, pages 2425–2432, 2018.
- [11] Misha Denil, Babak Shakibi, Laurent Dinh, Nando de Freitas, et al. Predicting parameters in deep learning. In *Advances in Neural Information Processing Systems (NIPS)*, pages 2148–2156, 2013.
- [12] Max Jaderberg, Andrea Vedaldi, and Andrew Zisserman. Speeding up convolutional neural networks with low rank expansions. *arXiv preprint arXiv:1405.3866*, 2014.
- [13] Yong-Deok Kim, Eunhyeok Park, Sungjoo Yoo, Taelim Choi, Lu Yang, and Dongjun Shin. Compression of deep convolutional neural networks for fast and low power mobile applications. In *Proceedings of the International Conference on Learning Representations (ICLR)*, May 2016.
- [14] Marcella Astrid and Seung-Ik Lee. Cp-decomposition with tensor power method for convolutional neural networks compression. In *Big Data and Smart Computing (BigComp), 2017 IEEE International Conference on*, pages 115–118. IEEE, 2017.
- [15] Vadim Lebedev, Yaroslav Ganin, Maksim Rakhuba, Ivan Oseledets, and Victor Lempitsky. Speeding-up convolutional neural networks using fine-tuned cp-decomposition. *arXiv preprint arXiv:1412.6553*, 2014.
- [16] Xiangyu Zhang, Jianhua Zou, Kaiming He, and Jian Sun. Accelerating very deep convolutional networks for classification and detection. *IEEE transactions on pattern analysis and machine intelligence*, 38(10):1943–1955, 2016.
- [17] Yihui He and Song Han. Adc: Automated deep compression and acceleration with reinforcement learning. *arXiv preprint arXiv:1802.03494*, 2018.
- [18] Hyeji Kim and Chong-Min Kyung. Automatic rank selection for high-speed convolutional neural network. *arXiv preprint arXiv:1806.10821*, 2018.
- [19] Shinichi Nakajima, Masashi Sugiyama, S Derin Babacan, and Ryota Tomioka. Global analytic solution of fully-observed variational bayesian matrix factorization. *Journal of Machine Learning Research*, 14(Jan):1–37, 2013.
- [20] Alex Krizhevsky, Ilya Sutskever, and Geoffrey E Hinton. Imagenet classification with deep convolutional neural networks. In *Advances in neural information processing systems*, pages 1097–1105, 2012.
- [21] Karen Simonyan and Andrew Zisserman. Very deep convolutional networks for large-scale image recognition. In *Proceedings of the International Conference on Learning Representations (ICLR)*, May 2015.
- [22] Kaiming He, Xiangyu Zhang, Shaoqing Ren, and Jian Sun. Deep residual learning for image recognition. In *Proceedings of the IEEE conference on computer vision and pattern recognition*, pages 770–778, 2016.
- [23] Jia Deng, Wei Dong, Richard Socher, Li-Jia Li, Kai Li, and Li Fei-Fei. Imagenet: A large-scale hierarchical image database. In *Computer Vision and Pattern Recognition, 2009. CVPR 2009. IEEE Conference on*, pages 248–255. IEEE, 2009.
- [24] Alex Krizhevsky and Geoffrey Hinton. Learning multiple layers of features from tiny images. Technical report, Citeseer, 2009.
- [25] Yangqing Jia, Evan Shelhamer, Jeff Donahue, Sergey Karayev, Jonathan Long, Ross Girshick, Sergio Guadarrama, and Trevor Darrell. Caffe: Convolutional architecture for fast feature embedding. In *Proceedings of the 22nd ACM international conference on Multimedia*, pages 675–678. ACM, 2014.